Mechanics Research Communications 58 (2014) 17–23

Contents lists available at ScienceDirect

Mechanics Research Communications

journal homepage: www.elsevier.com/locate/mechrescom

Mechanics of collagen–hydroxyapatite model nanocomposites

Flavia Libonati[a,b], Arun K. Nair[b], Laura Vergani[a], Markus J. Buehler[b,*]

[a] Politecnico di Milano, via G. La Masa 1, 20156 Milano, Italy
[b] Civil and Environmental Engineering, Massachusetts Institute of Technology, 77th Massachusetts Avenue, Cambridge, United States

ARTICLE INFO

Article history:
Received 9 May 2013
Accepted 19 August 2013
Available online 29 August 2013

Keywords:
Bone
Materiomics nanocomposites
Nanomechanics
Atomistic, Collagen
Hydroxyapatite

ABSTRACT

Bone is a hierarchical biological composite made of a mineral component (hydroxyapatite crystals) and an organic part (collagen molecules). Small-scale deformation phenomena that occur in bone are thought to have a significant influence on the large scale behavior of this material. However, the nanoscale behavior of collagen–hydroxyapatite composites is still relatively poorly understood. Here we present a molecular dynamics study of a bone model nanocomposite that consist of a simple sandwich structure of collagen and hydroxyapatite, exposed to shear-dominated loading. We assess how the geometry of the composite enhances the strength, stiffness and capacity to dissipate mechanical energy. We find that H-bonds between collagen and hydroxyapatite play an important role in increasing the resistance against catastrophic failure by increasing the fracture energy through a stick-slip mechanism.

1. Introduction

Bone is a structural biological composite made of a mineral part, consisting of hydroxyapatite (also abbreviated as HAP) mineral crystals, and an organic part, consisting of collagen molecules. Hydroxyapatite and collagen represent the basic building blocks of bone that are arranged at various length-scales to form a complex hierarchical structure (Alexander et al., 2012; Espinosa et al., 2009; Fratzl et al., 2004; Launey et al., 2010; Ritchie et al., 2009; Nair et al., 2013; Weiner and Wagner, 1998). At small scales, the confined size of its building blocks has been shown to be an important element in reaching its characteristic mechanical properties (Gao et al., 2003b; Launey et al., 2010). Although bone has been quite widely studied in the literature, the behavior of collagen–hydroxyapatite nanocomposite is still relatively poorly understood, in particular from an atomistic perspective. The combination of full atomistic modeling techniques and coarse grain modeling can be succesfully applied to describe collagenous tissues and bone from a fundamental point of view (Buehler, 2006, 2007, 2008; Buehler et al., 2006; Gautieri et al., 2009a; Nair et al., 2013). In Table 1, we present an overview of the mechanical properties of collagen, hydroxyapatite and collagen–hydroxyapatite nanocomposites, by collecting literature data from both experiments and simulations.

In this paper, we present a study of hydroxyapatite–collagen composites from an atomistic viewpoint, and carry out a series of simulations to assess the behavior of bone's elementary building blocks and their interactions. We focus on simple sandwich structures that consist of collagen and hydroxyapatite, and expose them to shear dominated loading. We investigate the behavior of the interface at the level of the chemical interactions (across the interface), and identify deformation mechanisms to explain different mechanical signatures associated with them. We carry out simulations in both dry and wet conditions, to understand the effect of water on the mechanical properties of the nanocomposites, and also investigate the effect of confining the size of the systems on the overall mechanical response.

The computational model is designed to shed light on the mechanical behavior and deformation mechanisms of a composite system containing a single tropocollagen molecule and two crystals of hydroxyapatite. Our model is meant to be simple and not meant to be an accurate representation of the actual bone nanostructure. Rather, it should help us to identify deformation and toughnening mechanisms at the nanoscale, and reveal how these mechanisms can possibly influence bone's larger-scale mechanical properties (e.g. in the context of fracture process zones). Hence, this study is important for modeling bone composite from the bottom up and can pave the way to study more complex bone biological composites. The understanding of such phenomena may provide important information for the study of bone and for the design of bone-like materials, by mimicking relevant mechanisms.

2. Materials and methods

2.1. Atomistic model of collagen and hydroxyapatite

Our model is a composite sandwich structure, consisting of two outer layers of hydroxyapatite and an internal layer of collagen.

* Corresponding author. Tel.: +1 617 452 2750.
E-mail address: mbuehler@MIT.EDU (M.J. Buehler).

0093-6413/$ – see front matter © 2013 Elsevier Ltd. All rights reserved.
http://dx.doi.org/10.1016/j.mechrescom.2013.08.008

Table 1
Mechanical properties of collagen, hydroxyapatite, and hydroxyapatite–collagen composites from literature data (experiments and simulations).

Material	Method	Tensile modulus [GPa]	Extensibility [%]	Tensile strength [GPa]
Tropocollagen molecule	Experiment (Sun et al., 2004)	0.35–12	30	–
Tropocollagen molecule	Simulation (Buehler, 2006)	1.8–4	50	10.96
Hydroxyapatite	Experiment (Gilmore and Katz, 1982)	114	–	–
Hydroxyapatite	Simulation (Ching et al., 2009)	120.6	10–16 (perfect crystal)	7.4–9.6
Hydroxyapatite–collagen composite	Simulation (Qin et al., 2012)	30.16–31.87	N/A	19.37–21.41

Table 2
Geometrical and mechanical properties of hydroxyapatite–collagen nanocomposites (*i.e.* sandwich structures) determined from the simulations. The interlayer distance is measured after the structure relaxation.

Structure	Condition	Interlayer distance, d [nm]	Maximum force [N]·10^{-8}	Tensile strength [GPa]	Shear strength [GPa]	Stiffness [N/m]
Initial	Dry	2.6	5.91	33.42	0.81	3.22
Initial	Wet	4.1	6.81	38.56	0.93	6.36
Confined	Dry	1.9	7.60	42.99	1.04	5.44
Confined	Wet	2.5	7.20	40.76	0.98	6.29

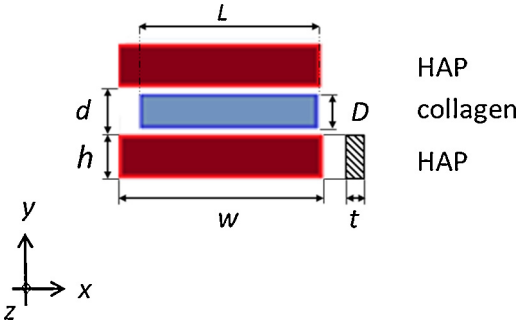

Fig. 1. Geometry and dimensions of the sandwich models used in our atomistic study. Different samples are created by varying the interlayer distance, '*d*'.

The slabs of hydroxyapatite are aligned with the *c*-axis of the crystal (*i.e.* along the [1 0 0] direction) parallel to the main axis of the collagen molecule (the hydroxyapatite basal plane (0 0 1) lies in the *xy*-plane). The top and bottom layers of hydroxyapatite have the same geometry and dimensions: width, $w \approx 19.2$ nm, height, $h \approx 1.6$ nm, and thickness, $t \approx 2.8$ nm; the end-to-end distance of the collagen molecule is, $L \approx 14.9$ nm and the diameter of the triple helical structure, $D \approx 1.5$ nm. All above mentioned parameters are kept fixed during all the simulations, whereas we vary the *y*-distance between the two layers of hydroxyapatite, here referred to as 'interlayer distance' and indicated with *d*. Fig. 1 shows the model with parameters such as height, width, thickness, diameter, length, and interlayer distance. In Fig. 2, we depict a snapshot of a sandwich model and emphasize the molecular structure of the basic features, such as the hydroxyapatite unit cell and the collagen pro-α chains and amino-acid chains. The values of the interlayer distance are given in Table 2.

2.1.1. Crystal geometry

We generate the hydroxyapatite crystal unit cell using Materials Studio 4.4 (Accelrys, Inc.). It is a hexagonal unit cell (HCP lattice) with 44 atoms and the following lattice parameters: $a = 9.4241$ Å, $b = 9.4241$ Å, $c = 6.8814$ Å, $\alpha = 90°$, $\beta = 90°$, $\gamma = 120°$ (Libonati et al., 2013; Qin et al., 2012). The samples are created by replicating the unit cell 20 times in the *x* directions, two times in the *y* direction, and four times in the *z* directions.

We focus on the interaction with the (0 1 0) plane, which plays an important role in the morphology of biological materials, and in particular during the biomineralization process, owing to the collagen-driven growing effect. Moreover, it has electrostatic characteristics on its surfaces, showing a negative charge on the OH-rich surface and a positive charge on the Ca-rich surface; (1 0 0) plane is the most stable and it has geometrical and chemical similarity to the (0 1 0) plane, whereas the (0 0 1) plane is neutral (Astala and Stott, 2008; Olszta et al., 2007; Qin et al., 2012). In this study we investigate the interactions between the collagen molecule and the OH-rich surface of the hydroxyapatite (0 1 0) plane, as it ensures a stronger adhesion than the Ca-rich one (Qin et al., 2012). This is due to the OH-rich groups, which provide more donors and acceptors for the formation of H-bonds with the collagen molecule.

2.1.2. Protein model

For the protein model, we use a tropocollagen molecule previously equilibrated in an *NPT* ensemble (Chang et al., 2012). Indeed, in the earlier work (Chang et al., 2012) the

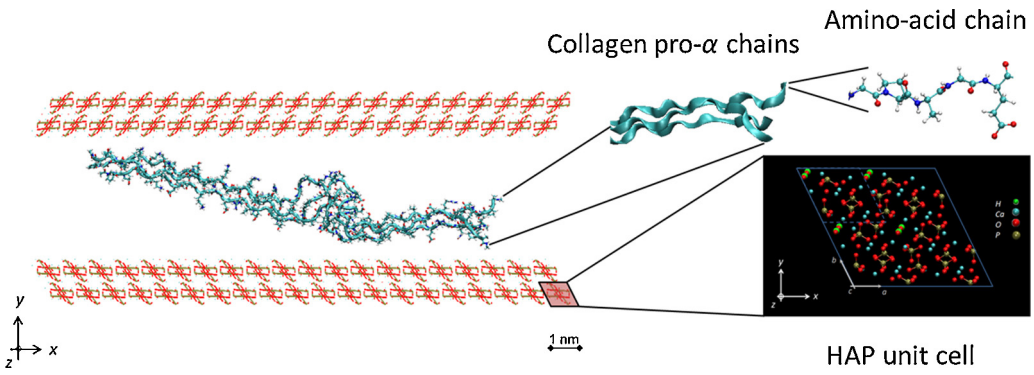

Fig. 2. Snapshot of the collagen–hydroxyapatite nanocomposite investigated in this study. The building blocks (the hydroxyapatite unit cell, the collagen pro-α chains and amino-acid chains) are visualized on the right.

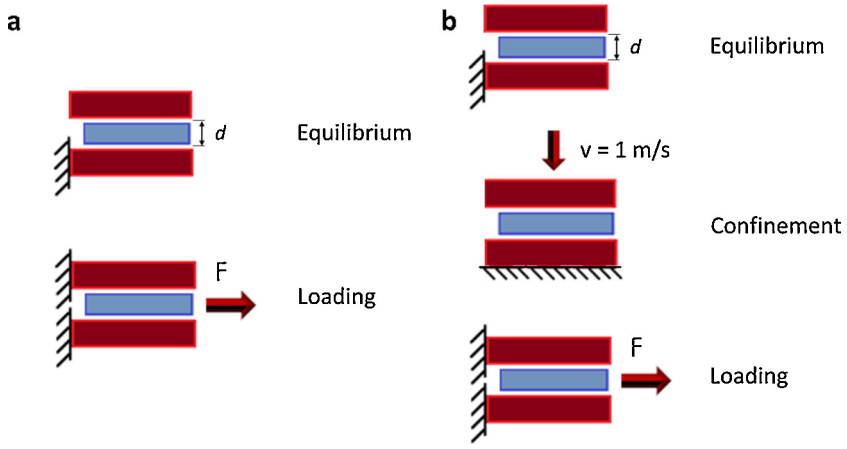

Fig. 3. Simulation setups used in this study. (a) Simulation scheme for the initial case: boundary and loading conditions during the equilibrium and loading phase. (b) Simulation scheme for the confined case: boundary and loading conditions during the equilibrium, the confinement, and the stretching phase.

authors used the real sequences of type I α-1 and type I α-2 chains of *mus musculus* (wild type mouse), taken from the National Center for Biotechnology Information protein database (http://www.ncbi.nlm.nih.gov/protein) and created the collagen molecules by inputting the sequences of three chains into the software THeBuScr (Triple-Helical collagen Building Script) (Rainey and Goh, 2004). The two chains (α-1 and α-2) include 1014 residues with repeated G–X–Y triplets, except the C-terminal and N-terminal sequences. However, to reduce the computational costs, Chang et al. focused on a specific section, including 57 residues (from the 403rd to 459th position) to generate the heterotrimer collagen molecule. This choice ensures that the amino acid composition (by %) of the segment is similar to the composition of the complete collagen molecule, and that the six residues of the α-1 and α-2 chains are the same, avoiding any boundary effect. The detailed sequence of the modeled segment is given in the original paper (Chang et al., 2012).

2.1.3. Force field

In this work we use an extended CHARMM force field as reported in (Qin et al., 2012), because it has been shown to correctly model the behavior of collagen and hydroxyapatite–collagen systems. Qin et al. included parameters derived from quantum mechanics calculations (Park et al., 2005) for hydroxyproline (HYP), a nonessential amino acid typical of collagen but not present in other proteins, and added nonbonded parameters, calculated by using a Born–Mayer–Huggins model (Bhowmik et al., 2007; Hauptmann et al., 2003). The bond, angle and dihedral parameters were derived from both quantum-mechanics calculations and experimental data. The force field has been validated in earlier works (Bhowmik et al., 2007; Dubey and Tomar, 2009; Hauptmann et al., 2003; Qin et al., 2012; Shen et al., 2008).

2.1.4. Steered molecular dynamics simulations

We carry out steered molecular dynamics (SMD) simulations by using the LAMMPS code (Plimpton, 1995). To describe the overall strain energy of the system we adopt a modified CHARMM force field, where Lennard–Jones and Coulombic interactions are computed with an additional switching function that ramps the energy and force smoothly to zero between an inner and outer cutoff, of 8 Å and 10 Å, respectively (Plimpton, 1995). This cutoff range is selected to include one unit lattice over the thickness. An additional $1/r$ term is also included in the Coulombic formula, making the Coulombic energy varying as $1/r^2$, which is an effective distance-dielectric term. This represents a simple model for an implicit solvent with additional screening and it is designed to be used in simulations of biomolecules without explicit water solvent (Plimpton, 1995). However, we also investigate the effect of water. In this case, we use the VMD (Visual Molecular Dynamics) software (Humphrey et al., 1996) to solvate the structure, including it in a larger water box of TIP3 water molecules. The structure in explicit solvent is then included in a large simulation box with fixed (non-periodic) boundary conditions.

The initial structure is geometrically optimized through energy minimization, by using two different algorithms, the conjugate gradient and the steepest descent methods. Afterwards we clamp the left edge of the hydroxyapatite bottom layer and relax the structure under an *NVE* ensemble for 2 ns. We set the temperature to 300 K by using a Langevin thermostat. Once the structure is fully relaxed (confirmed by the root-mean square deviation convergence to a constant value), we perform SMD simulations: we constraint the left edges of the two hydroxyapatite layers and we apply load to the right-end part of the collagen, by pulling the center of mass of the terminal α-carbon atoms of the collagen pro α-chains via a virtual spring, with an elastic

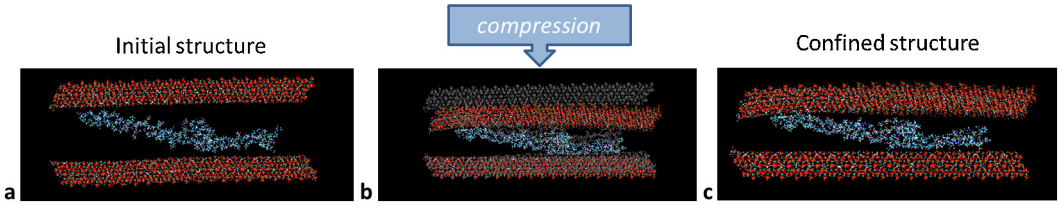

Fig. 4. Snapshots of deformation. (a) Visualization of the final equilibrated structure, before the confinement phase. (b) Snapshot of the confinement phase. The hydroxyapatite top layer before and after confinement are represented in gray color and red color, respectively, to show the difference in position. (c) Final equilibrated structure, after the confinement phase. The confined structure shows a reduced interlayer distance (about 25% and 40% less than the initial ones, in dry and wet cases respectively). (For interpretation of the references to color in this text, the reader is referred to the web version of the article.)

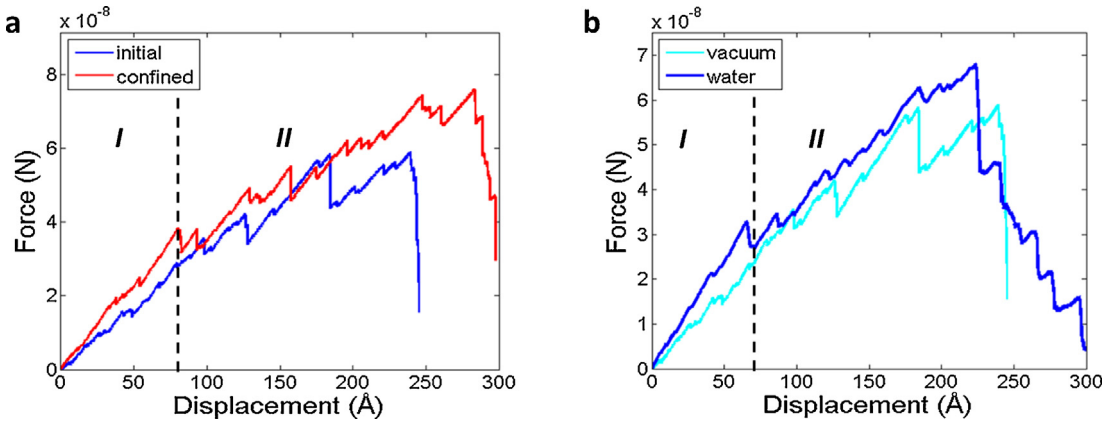

Fig. 5. Example of force–displacement curves. (a) Comparison between the initial structure (blue line) and the confined one (red line). The geometrically confined structure shows increased mechanical properties (*i.e.* stiffness and strength) compared to the initial case. (b) Comparison between a dry (light blue line) and wet case (blue line); the water causes a general increase in the mechanical properties (blu line), owing to the interactions of both the mineral and the protein with the water molecules. The curves are highly repeatable for all studied cases and characterized by an initial regime (regime I) with a linear trend and a secondary one (regime II) – with a nonlinear trend – until failure occurs. The black dashed line distinguishes the two regimes. (For interpretation of the references to color in this text, the reader is referred to the web version of the article.)

constant $k_{spring} = 8000\,kJ\,mol^{-1}\,nm^{-2}$. We set the pulling velocity to 0.01 Å/ps (1 m/s), similar to that used in previous studies (Gautieri et al., 2009b; Qin et al., 2012). The simulation setup is shown in Fig. 3a. A time step of 0.5 fs is used in all simulations presented here.

To investigate the effect of geometric confinement on the mechanics of the hydroxyapatite–collagen nanocomposites, we carry out simulations of a confined structure, characterized by a reduced interlayer distance. We expose the structure to increasing levels of confinement, previously equilibrated for 2 ns under an *NVE* ensemble and lead it to 300 K through a Langevin thermostat, by moving the hydroxyapatite top layer downwards, with a velocity of 1 (m/s) ('confinement phase'). We then apply the load as described above for the other case. In the confined cases, we also perform simulations in both dry and wet conditions. The simulation setup for the confined case is shown in Fig. 3b.

2.2. Data post-processing

We analyze the data by using VMD (Humphrey et al., 1996), allowing the visualization of the simulation trend, the test snapshots printing, and the computing of H-bonds. For the H-bond calculations we consider a donor–acceptor distance of 3.5 Å and an angle cutoff of 30°. To analyze the mechanical response of the system under the applied loading conditions, we use MATLAB (Mathworks, Inc.). To determine the mechanical properties under a mainly shear loading we use force–displacement data (*i.e.* stiffness, maximum force, tensile and shear strength, etc.). The displacement is calculated as the shift of the SMD loading point. To determine the stiffness we use a linear fitting to the force–displacement data, for displacement up to 2% of the total one. The tensile strength is calculated as the maximum force recorded during a simulation, divided by the collagen cross-section. This value may be representative of the strength of a collagen fibril, with the effect of the side hydroxyapatite layers, result that can be directly compared with those calculated earlier (Qin et al., 2012). Also, this value might be correlated with the strength of a mineralized collagen fibril. Moreover, by considering the sandwich models, above described, similar to the case of a double lap joint subjected to tensile loading, as described by the standard (ASTM, 2008), we can calculate the shear strength as defined in (ASTM, 2008), as the maximum force divided by the overlap area. In our study, we calculate the overlap area by considering the projection of the collagen (approximate to a cylinder) on the hydroxyapatite layers.

3. Results

We proceed with a systematic description of the results from our computational experiments. Fig. 4 depicts the final equilibrated structures, before and after the confinement phase. The confined structures show an interlayer distance of about 25% and 40% less than the initial ones, in dry and wet cases, respectively. We should stress that the relaxed structures are not completely flat, and hence the interlayer distance represents an average value. Indeed, we consider the distance between the two hydroxyapatite layers at three points along the *x*-direction and *d* as the average value. Values of *d* are given in Table 2, along with the mechanical properties resulted from the simulations. We calculate the tensile strength, considering the maximum force divided by the collagen cross-sectional area. The calculated tensile strength allows us to perform a comparison with earlier results reported in (Qin et al., 2012), where a collagen–hydroxyapatite nanocomposite similar to a single lap joint subject to tensile loading has been studied. The results show a stiffening effect, likely owing to the presence of a second layer of hydroxyapatite, and an increase in strength, which turns out to be twice the value calculated in (Qin et al., 2012). In Fig. 5a we depict a representative force–displacement graph, for both initial and confined case, showing that the geometric confinement causes a general increase of the mechanical properties (*i.e.* stiffness and strength). Fig. 5b depicts the curves for a dry and a solvated case, where the water leads to a general increase in the mechanical properties, owing to the interactions of both the mineral and the protein with the water molecules. The curves are repeatable for all the studied cases and characterized by an initial linear regime (regime I) and a secondary nonlinear one (regime II), until failure occurs. Both regimes are highlighted in Fig. 5. By following the molecular trajectories we identify the deformation mechanisms occurring during the simulations by visualizing the molecular structures at different deformation stages. These mechanisms can be summarized as follows:

- Breaking of atomic interactions (*i.e.* electrostatic and VdW interactions), between the collagen chains and between collagen and hydroxyapatite,

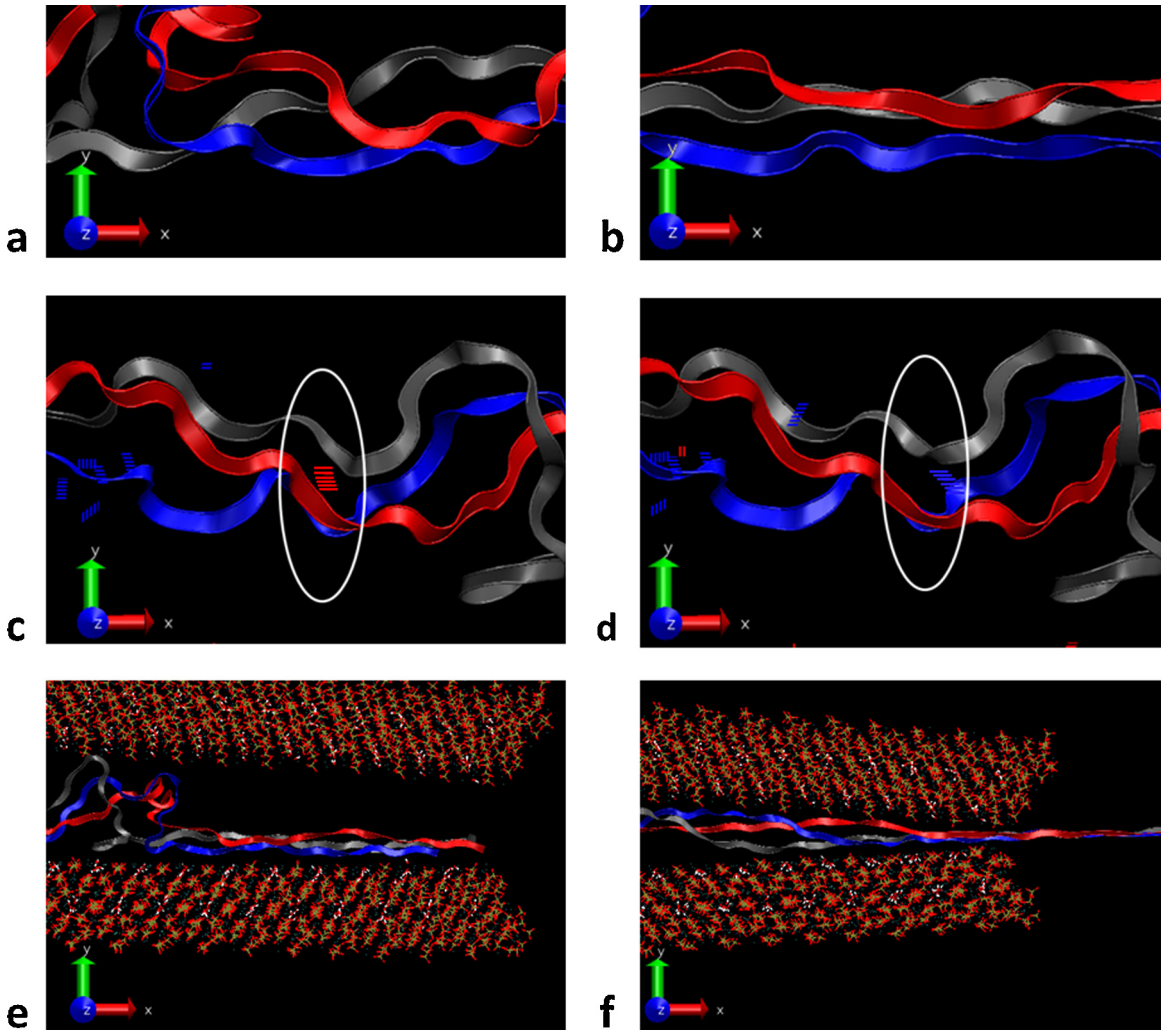

Fig. 6. Snapshots revealing the primary deformation mechanisms. (a and b) Chain uncoiling and unfolding in two consecutive steps, occurring due to breakage of intra-molecular H-bonds, which initially stabilize the collagen triple helix. (c and d) Intra-molecular H-bonds formation and breakage (in the first snapshot, panel c, an H-bond is highlighted with red lines; in the second snapshot, panel d, corresponding to the following frame, the previous H-bond is broken and a new one, represented with blue line, is formed). (d and e) Chain sliding and stretching: snapshots in panel e and panel f show how the collagen chains slides on the mineral surfaces and how it is stretched as the force is applied. (For interpretation of the references to color in this text, the reader is referred to the web version of the article.)

- Chain uncoiling and unfolding, due to the breakage of intra-molecular H-bonds, which initially stabilize the collagen triple helix, and
- Sliding of the collagen chains on the hydroxyapatite surface in a discontinuous way, owing to the progressive breakage of H-bonds.

Fig. 6a–f shows snapshots of the above mentioned deformation mechanisms.

In Fig. 7 we depict the number of H-bonds during the simulations for one of the studied cases. The plot shows the linear density of H-bonds (*i.e.* number of H-bonds normalized on the equilibrated length of the tropocollagen molecule) with respect to the shear displacement during the tests, including both intra-molecular (*i.e.* between individual tropocollagen chains) and inter-molecular (*i.e.* between the tropocollagen chains and the hydroxyapatite surface) H-bonds. These curves are similar for all the cases and characterized by a decreasing trend of intra-molecular H-bonding and an increasing trend of inter-molecular H-bonds, the latter followed by a bumpy region.

The intermolecular H-bonds play a major role in the interface strength of the studied nanocomposite system. By comparing the graphs in Figs. 5 and 7, we can explain the deformation mechanisms as follows. Initially, when the force–displacement trend is linear (regime I), chain unfolding and uncoiling, via intra-molecular H-bonds breakage occurs. Subsequently, continuous formation and breakage of inter-molecular H-bonds occurs, which facilitates protein sliding on the mineral surface in a discontinuous way, and hence increases the energy required to failure. The latter mechanism corresponds to regime II in the force–displacement graph (for displacements larger than 80 Å).

This trend is common to all the studied structures, but less clear in the solvated cases than the dry ones, due to the water-mediated effect (*i.e.* H-bonds form with water molecules also). Indeed, the presence of water, which interacts with both collagen and hydroxyapatite, reduces the direct coupling between the protein and the mineral. This concept has also been shown in previous studies (Gupta et al., 2006), where "sacrificial bonds" such as H-bonds have been shown to play a crucial role. In fact, the progressive formation and breakage of such bonds act as a significant energy dissipation mechanism, leading to an increase in toughness, especially in the confined structures. In all cases, final failure occurs by breakage of the tropocollagen molecule, being the weakest component, instead of the interface failure.

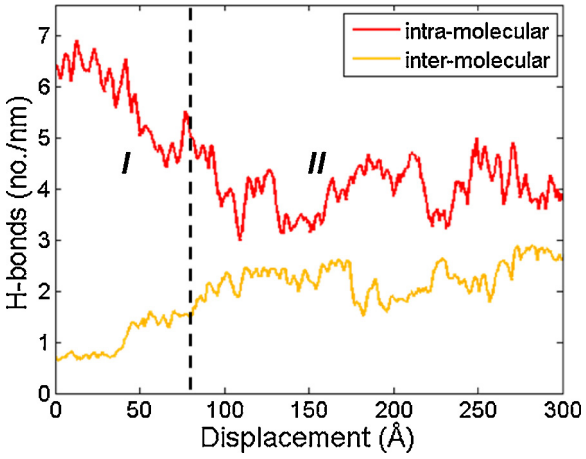

Fig. 7. A count of the H-bonds for one of the studied cases (for the confined case depicted in Fig. 5). Linear density of intra-molecular (red line) and inter-molecular (orange line) H-bonds (*i.e.* number of H-bonds normalized on the equilibrated length of the tropocollagen molecule) with respect to the shear displacement during the test. The H-bonds curves are characterized by a decreasing trend of intra-molecular H-bonds until a plateau has been reached, and an increasing trend of inter-molecular H-bonds, followed by a bumpy region. Intra-molecular H-bonds are progressively broken in regime I, allowing for collagen uncoiling and unfolding. Inter-molecular H-bonds continuously form and break allowing collagen sliding in a discontinuous way on the mineral surfaces. The black dashed line highlights the two regions: the initial linear regime I and the secondary regime II of the force–displacement trend depicted in Fig. 5. (For interpretation of the references to color in this text, the reader is referred to the web version of the article.)

4. Concluding remarks

We presented a study of collagen–hydroxyapatite nanocomposites from a simple, fundamental point of view. The results of the simulations show a force–displacement trend characterized by an initial linear regime (regime I), and a secondary nonlinear regime (regime II):

- In regime I, the primary deformation mechanisms are chain uncoiling and unfolding, due to the breakage of weak VdW interactions, electrostatic interactions and intra-molecular H-bonds. Indeed, when tropocollagen is straightened, different bonds break progressively. First, the weak VdW interactions, which requires low energy to be broken. Then, electrostatic interaction and intra-molecular H-bonds, which initially stabilize the collagen helical structure, gradually break until reaching a plateau. The small variation in the number of intra-molecular H-bonds is due to that they are continuously broken and reformed along the peptide axis, because the pro-alpha chains are close enough to form H-bonds, though the helical structure is lost.
- In regime II, the system reaches a steady state, and the number of intra-molecular H-bonds remains approximately constant. As the force is increased (for displacement larger than 80 Å), the two hydroxyapatite layers come closer to each other and interact increasingly with the collagen molecule. At this point, defomation occurs in a discontinuous way, mediated via inter-molecular H-bonds, which allow collagen chains stepwise sliding on the mineral surface. In the last stages, before reaching the maximum force backbone stretching occurs until catastrophic failure of the system.

In sum, we observed how the presence of hydroxyapatite increases the mechanical performance of the composite and how geometric confinement causes a general increase in the mechanical performance of the system. Indeed, according to previous studies, it is not only the structure of the building blocks that can explain the resilience of bone at the molecular level, but also their geometry. In particular, the nanoconfined size of bone's building blocks plays a main role in determining the mechanical properties of bone, leading to new phenomena that do not occur at larger scales (Gao et al., 2003a). Moreover, we observe the crucial role of inter-molecular H-bonds, which act as "sacrificial" bonds. Indeed, the progressive formation and breakage of such bonds increases the energy to failure, acting as a toughening mechanism. The mechanism of sacrificial bonds is one of the key mechanisms in bone nanocomposites and has been described in the literature, often as a result from large stresses in the process zone surrounding larger defects (Fantner et al., 2005; Launey et al., 2010; Ritchie et al., 2009; Smith et al., 1999). Our molecular study provides evidence for the possibility of such slip mechanisms, and quantifies possible chemical–mechanical processes that occur. These findings are consistent with existing experimental data. Future work could consider more realistic molecular models of bone, or focus on theoretical models that explore a wider range of structure–property-process relationships.

Acknowledgements

We acknowledge support from MIT-Italy Program ("Progetto Rocca"). High performance computing resources have been provided by CINECA, through the ISCRA initiative. We acknowledge support from NSF (grant number CMMI-0642545) and ONR (grant number N000141010562).

References

Alexander, B., Daulton, T.L., Genin, G.M., Lipner, J., Pasteris, J.D., Wopenka, B., Thomopoulos, S., 2012. The nanometre-scale physiology of bone: steric modelling and scanning transmission electron microscopy of collagen–mineral structure. Journal of the Royal Society Interface 9, 1774–1786.

Astala, R., Stott, M.J., 2008. First-principles study of hydroxyapatite surfaces and water adsorption. Physical Review B 78, 075427.

ASTM, 2008. ASTM D 3528-96 – Standard Test Method for Strength Properties of Double Lap Shear Adhesive Joints by Tension Loading.

Bhowmik, R., Katti, K.S., Katti, D., 2007. Molecular dynamics simulation of hydroxyapatite–polyacrylic acid interfaces. Polymer 48, 664–674.

Buehler, M.J., 2006. Atomistic and continuum modeling of mechanical properties of collagen: elasticity, fracture, and self-assembly. Journal of Materials Research 21, 1947–1961.

Buehler, M.J., 2007. Molecular nanomechanics of nascent bone: fibrillar toughening by mineralization. Nanotechnology 18, 295102.

Buehler, M.J., 2008. Nanomechanics of collagen fibrils under varying cross-link densities: atomistic and continuum studies. Journal of the Mechanical Behavior of Biomedical Materials 1, 59–67.

Buehler, M.J., Yao, H., Gao, H., Ji, B., 2006. Cracking and adhesion at small scales: atomistic and continuum studies of flaw tolerant nanostructures. Modelling and Simulation in Materials Science and Engineering 14, 799.

Chang, S.-W., Shefelbine, Sandra, J., Buehler, Markus, J., 2012. Structural and mechanical differences between collagen homo- and heterotrimers: relevance for the molecular origin of brittle bone disease. Biophysical Journal 102, 640–648.

Ching, W.Y., Rulis, P., Misra, A., 2009. Ab initio elastic properties and tensile strength of crystalline hydroxyapatite. Acta Biomaterialia 5, 3067–3075.

Dubey, D.K., Tomar, V., 2009. Role of the nanoscale interfacial arrangement in mechanical strength of tropocollagen–hydroxyapatite-based hard biomaterials. Acta Biomaterialia 5, 2704–2716.

Espinosa, H.D., Rim, J.E., Barthelat, F., Buehler, M.J., 2009. Merger of structure and material in nacre and bone – perspectives on de novo biomimetic materials. Progress in Materials Science 54, 1059–1100.

Fantner, G.E., Hassenkam, T., Kindt, J.H., Weaver, J.C., Birkedal, H., Pechenik, L., Cutroni, J.A., Cidade, G.A.G., Stucky, G.D., Morse, D.E., Hansma, P.K., 2005. Sacrificial bonds and hidden length dissipate energy as mineralized fibrils separate during bone fracture. Nature Materials 4, 612–616.

Fratzl, P., Gupta, H.S., Paschalis, E.P., Roschger, P., 2004. Structure and mechanical quality of the collagen–mineral nano-composite in bone. Journal of Materials Chemistry 14, 2115–2123.

Gao, H., Ji, B., Jager, I.L., Arzt, E., Fratzl, P., 2003a. Materials become insensitive to flaws at nanoscale: lessons from nature. Proceedings of the National Academy of Sciences 100, 5597–5600.

Gao, H., Ji, B., Jäger, I.L., Arzt, E., Fratzl, P., 2003b. Materials become insensitive to flaws at nanoscale: lessons from nature. Proceedings of the National Academy of Sciences 100, 5597–5600.

Gautieri, A., Uzel, S., Vesentini, S., Redaelli, A., Buehler, M.J., 2009a. Molecular and mesoscale mechanisms of osteogenesis imperfecta disease in collagen fibrils. Biophysical Journal 97, 857–865.

Gautieri, A., Vesentini, S., Redaelli, A., Buehler, M.J., 2009b. Intermolecular slip mechanism in tropocollagen nanofibrils. Journal of Materials Research, 921–925.
Gilmore, R.S., Katz, J.L., 1982. Elastic properties of apatites. Journal of Materials Science 17, 1131–1141.
Gupta, H.S., Seto, J., Wagermaier, W., Zaslansky, P., Boesecke, P., Fratzl, P., 2006. Cooperative deformation of mineral and collagen in bone at the nanoscale. Proceedings of the National Academy of Sciences 103, 17741.
Hauptmann, S., Dufner, H., Brickmann, J., Kast, S.M., Berry, R.S., 2003. Potential energy function for apatites. Physical Chemistry Chemical Physics 5, 635–639.
Humphrey, W., Dalke, A., Schulten, K., 1996. VMD: visual molecular dynamics. Journal of Molecular Graphics 14, 33–38.
Launey, M.E., Buehler, M.J., Ritchie, R.O., 2010. On the mechanistic origins of toughness in bone. Annual Review of Materials Research 40, 25–53.
Libonati, F., Nair, A.K., Vergani, L., Buehler, M.J., 2013. Fracture mechanics of hydroxyapatite single crystals under geometric confinement. Journal of the Mechanical Behavior of Biomedical Materials 20, 184–191.
Nair, A.K., Gautieri, A., Chang, S.W., Buehler, M.J., 2013. Molecular mechanics of mineralized collagen fibrils in bone. Nature Communications 4 (paper number 1724).
Olszta, M.J., Cheng, X., Jee, S.S., Kumar, R., Kim, Y.-Y., Kaufman, M.J., Douglas, E.P., Gower, L.B., 2007. Bone structure and formation: a new perspective. Materials Science and Engineering: R: Reports 58, 77–116.
Park, S., Radmer, R.J., Klein, T.E., Pande, V.S., 2005. A new set of molecular mechanics parameters for hydroxyproline and its use in molecular dynamics simulations of collagen-like peptides. Journal of Computational Chemistry 26, 1612–1616.
Plimpton, S., 1995. Fast parallel algorithms for short-range molecular dynamics. Journal of Computational Physics 117, 1–19.
Qin, Z., Gautieri, A.K., Nair, A., Inbar, H., Buehler, M.J., 2012. Thickness of hydroxyapatite nanocrystal controls mechanical properties of the collagen–hydroxyapatite interface. Langmuir 28, 1982–1992.
Rainey, J.K., Goh, M.C., 2004. An interactive triple-helical collagen builder. Bioinformatics 20, 2458–2459.
Ritchie, R.O., Buehler, M.J., Hansma, P., 2009. Plasticity and toughness in bone. Physics Today 62, 41–47.
Shen, J.W., Wu, T., Wang, Q., Pan, H.H., 2008. Molecular simulation of protein adsorption and desorption on hydroxyapatite surfaces. Biomaterials 29, 513–532.
Smith, B.L., Schaffer, T.E., Viani, M., Thompson, J.B., Frederick, N.A., 1999. Molecular mechanistic origin of the toughness of natural adhesives, fibres and composites. Nature 399, 761.
Sun, Y.-L., Luo, Z.-P., Fertala, A., An, K.-N., 2004. Stretching type II collagen with optical tweezers. Journal of Biomechanics 37, 1665–1669.
Weiner, S., Wagner, H.D., 1998. The material bone: structure mechanical function relations. Annual Review of Materials Science 28, 271–298.